

## **Air Assisted Atomization in Spiral Type Nozzles**

W. Kalata<sup>\*</sup>, K. J. Brown, and R. J. Schick  
Spray Analysis and Research Services  
Spraying System Co.  
Wheaton, IL 60187-7901 USA

### **Abstract**

Processes utilizing various spraying cooling are widely used in many gas treatment applications. Effective spray cooling system design optimization often depends on the approach used to investigate such gas cooling problems. The mass transfer efficiency of spray cooling problems depends on the ability of the liquid to atomize and disperse into the gas by interacting in a controlled manner. Experimental methods coupled with Computation Fluid Dynamics (CFD) can be used effectively in application design of a certain classes of spray evaporation processes.

In this study, a spiral type nozzle was studied. Both water and air flow at different respective mass fractions (mass flow rate of water over mass flow rate of air) were included while keeping the water flow the same. Phase Doppler Interferometry (PDI) and Laser Sheet Imaging (LSI) were used to measure the drop size and distribution throughout the range of operation conditions. The results indicated a slight reduction in drop size as air mass flow rate was increased. Additionally the increase in air flow caused a shift of the spray plume from predefined center axis.

At the same flow conditions, an internal and external two-phase flow of the nozzle was simulated with a Volume of Fluid (VOF) model which is a Computation Fluid Dynamics (CFD) method for multiphase problems. The fluids' velocity environment at the nozzle's orifice was investigated. As expected, the exit (from nozzle's orifice) velocities of the liquid increased as the mass fraction decreased due to increased total volume flow rate of both fluids.

---

<sup>\*</sup>Corresponding author: [wojciech.kalata@spray.com](mailto:wojciech.kalata@spray.com)

## Introduction

Global demand for gas fuels is expected to expand significantly as more nations adopt environmentally cleaner fuels to meet future economic growth and prioritize alternatives to minimize the impact of increasing oil-based energy costs. The environmental benefits of natural gas are clear. Burning gas emits fewer carbon emissions than burning coal or oil.

Various gases must be transported over long distances and maintained. Cooling gases in such lines is one of the methods to keep gases at proper conditions. Flashing off the gases from the liquid phase prior the injection into the main gas lines is a common occurrence and it has to be dealt with. This process requires further analysis, improvement and optimization. The improvements made in nozzle design and liquid atomization process in recent years have provided the possibility of process optimization towards an improvement of transport efficiency.

The combination of various testing techniques with computational fluid dynamics (CFD) allows for a rigorous engineering assessment and design of spray based systems. The focus of the present study was to analyze the effect of presence of the gas phase in a spiral type nozzle spray injection. For various air-water mixtures, this study investigated drop size, droplet velocities and spray patterns that were obtained experimentally. Additionally, CFD was performed to analyze the velocity environment at the nozzle's orifice at the same mixture conditions.

## Methods

### Process Conditions

The experimental setup consisted of a spiral-type hollow cone nozzle (Spraying Systems Co., 3/8BSJ-6030 as shown in Figure 1) spraying water along with assistance of air. The water flow was kept constant with changing air flow rate. All tests were carried out

spraying vertically downward into air as shown in Figure 2. The operating parameters for all tests are noted in Table 1. Note that a hydraulic case was added as a reference with a "typical" spray condition which this spiral nozzle was designed. It is important to note, that the air-assisted conditions had one-order of magnitude smaller liquid flow rate than the hydraulic reference case.

### Phase Doppler Interferometry

The Phase Doppler Interferometry (PDI) system used in this study was the Artium PDI 2D MD instrument with the integrated AIMS software used for automated processor setup. This technique measures the droplet size, velocity, angle of trajectory, and time of arrival of each particle passing through an optical measurement volume formed by pairs of intersecting laser beams. The technical explanation of the Phase Doppler technique can be reviewed in a number of publications including Bachalo et al. [1,2].

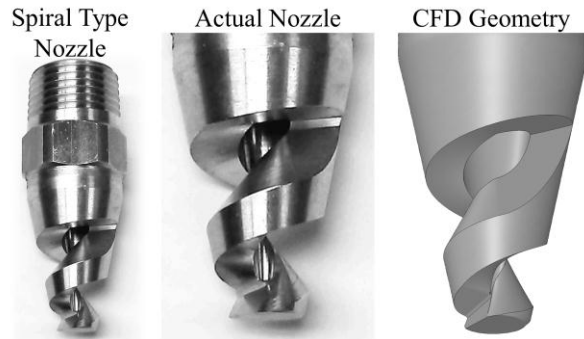


**Figure 1.** Spiral type spray nozzle (actual nozzle – left and middle, CFD geometry – right).

The ability to measure accurately requires the reliable characterization of the size, velocity, and transit

Parameter	Units	Hydraulic*	5% Mass Air	10% Mass Air	20% Mass Air
Water Flow Rate	L/min	17.11	1.893	1.893	1.893
Water Mass Flow Rate	kg/s	2.847E-01	3.149E-02	3.149E-02	3.149E-02
Air Flow Rate	Nm <sup>3</sup> /hr	0	5.097	10.19	20.39
Air Mass Flow Rate	kg/s	0	1.732E-03	3.465E-03	6.929E-03
Air/Water Mass Ratio (AWMR)		0	0.055	0.110	0.220

\*Hydraulic case was performed at increased flow rate to get equivalent drop size reading as compared to air-assisted cases.

**Table 1.** Experimental flow rate measurements.

time of each droplet. The PDI system is a validated method for droplet size and velocity measurement. Additionally, spray concentration measurements are possible, see Bade et al. [3,4].

The drop size and velocity measurements were performed 30.5 cm from the tip of the nozzle as shown in Figure 3. An intersection point of the x and y axes was directly underneath the center of the nozzle.

### Laser Sheet Imaging

The laser sheet imaging system implemented in this study was a DaVis image acquisition and processing software. The LSI system utilizes a laser sheet, with a Gaussian intensity profile, which illuminated the spray in a *single* downstream plane. The Gaussian intensity profile of the laser sheet is characterized and corrected for by imaging uniformly sized fog droplets over the entire image area. The laser sheet is approximately 1 mm thick which is sufficiently thin to represent a two dimensional sheet in the spray (z) direction, with images acquired in the x-y plane. The camera was located at an off-axis angle as shown in Figure 4. The image calibration was conducted by first imaging a calibration-sheet with markings of known size and spacing to characterize and correct the skewed camera images to the actual planar spray cross-section plane.

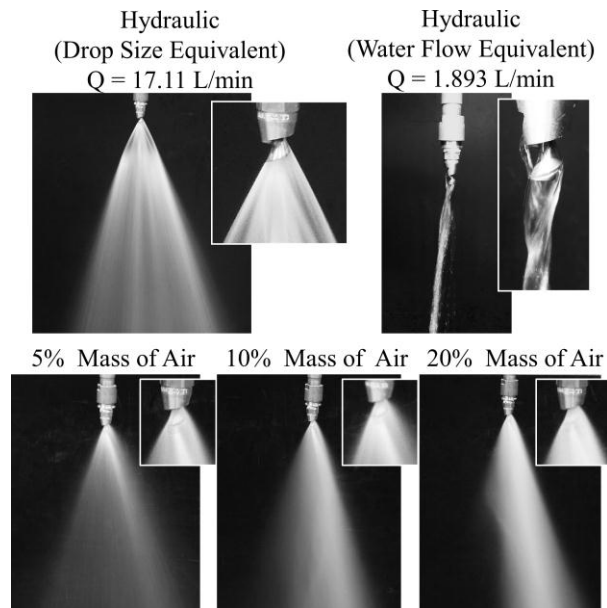


**Figure 2.** Spray from a spiral type nozzle at different air/water mass fraction cases.

In order to determine time-averaged spray coverage and shape information at each measurement, a minimum of 500 instantaneous (very short exposure time)

images are acquired, and the average of all 500 planar intensity distributions is taken. It is important to note that the resultant mean images are representative of the average light intensity scattered through Mie scattering, but not droplets across the image plane. Over each image's exposure time, each droplet that passes through the laser sheet will scatter light relative to its surface area. On average, the two-dimensional contours are therefore representative of the total surface area of droplets, which is a coupled to the result that is related by an increase in the number of droplets and/or larger droplets.

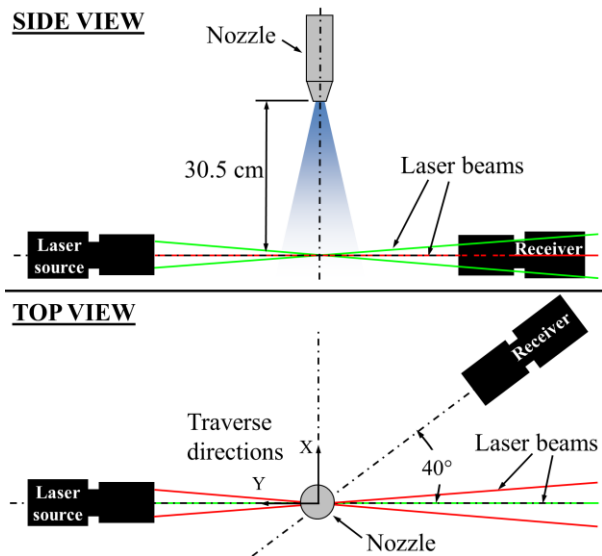


**Figure 3.** Setup for the PDI measurements.

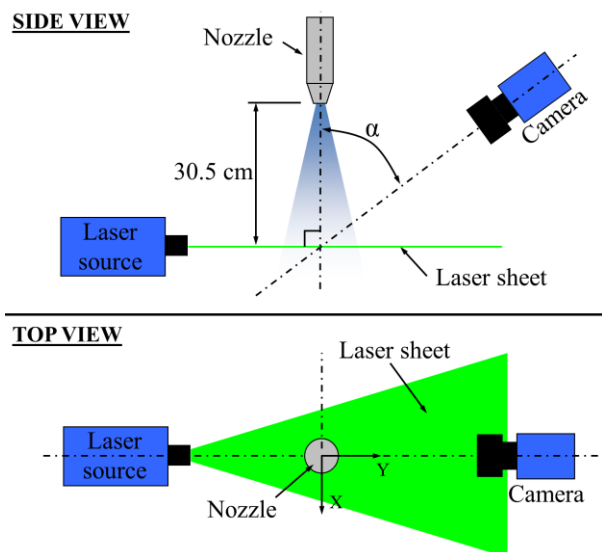


**Figure 4.** Setup for the LSI measurements.

Ultimately, these results provide good information on the coverage and shape of the spray cross-section, and slightly less useful information on the surface area distribution, rather than a more used volume distribution, although there is still good qualitatively relevant information in it.

The spray intensity profiles were measured similarly to PDI measurements. These profiles were obtained 30.5 cm from the tip of the nozzle as shown in Figure 4. An intersection point of x and y-axes was directly underneath the center of the nozzle. This time the coordinate system indicating positive x-y positioning was rotated 180 degrees.

### Computational Setup

CFD simulations were performed with ANSYS FLUENT version 14.5. The CFD model was reproduced according to the testing conditions where the nozzle orientation was aligned with experimental conditions. The geometry of the nozzle which is complicated due to helical structures was reproduced in 3-D modeler (Autodesk Inventor 2013). This geometry is shown in the right side of Figure 1. Meshing was performed within ANSYS Workbench 14.5 using the automated meshing tool. Initially, an unstructured grid was composed of 8.903 million mixed cells which employed boundary layer type inflation at all walls and utilized sizing function at the helical surfaces of the nozzle. Inside FLUENT, the unstructured mesh was converted into polyhedral grid while the boundary layer mesh remained. The grid was reduced to 2.114 million polyhedral cells.

Each CFD case was set up identically with liquid and air mass flow at inlet boundary condition (BC). As noted previously, liquid mass flow rate was kept constant. The air mass flow rate was changing accordingly to experimental setup (see Tables 1 and 2). The outlet pressure BC was setup as constant zero pressure with standard 1 bar operating pressure and properly setup gravity term. Nozzle walls were set as rigid, with no-slip conditions. The density of water and air were constant (998.2 and 1.225 kg/m<sup>3</sup> respectively) omitting a fact that at higher air to water mass ratio, the compressibility of air may be play additional role in changing the atomization process for this nozzle. Throughout all simulations, along with Volume of Fluid (VOF) model, the k-ε Realizable Turbulence Model with Standard

Wall Treatment was used. The simulations were performed in steady state mode [5], which lead to an implicit scheme for VOF model. The gradients were solved using Least Squares Cell Based method. The Second Order Upwind discretization scheme was used for Momentum, Volume Fraction, and Turbulence, while the spatial discretization used for pressure was set to PRESTO!. SIMPLE scheme was used for Pressure-Velocity Coupling.

### Experimental Results

As it was expected, the smallest relative overall drop-size was for the highest air/water mass ratio (AWMR) case, or in another words, as the largest volume of air was forced through the nozzle (see Figure 5). Overall Sauter Mean Diameter (SMD) was 97, 113, 122 and 141 microns for 20%, 10%, 5% AWMR and hydraulic cases respectively. The Median Volume Diameter (VMD) also expressed as  $D_{V0.5}$  was 104, 121, 131 and 160 for 20%, 10%, 5% AWMR and hydraulic cases respectively.

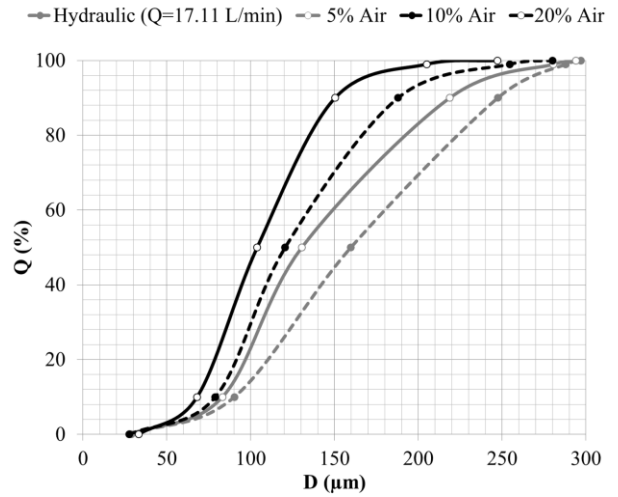
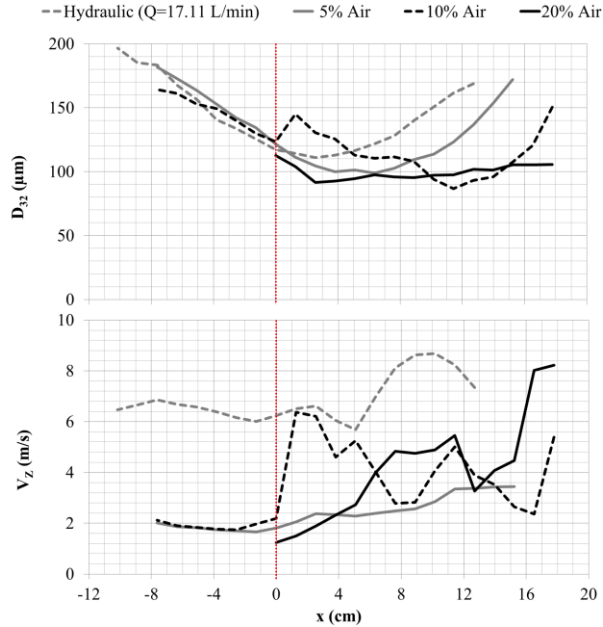


Figure 5. Overall drop size distributions for all cases.

Parameter	Units	5%	10%	20%
		Mass Air	Mass Air	Mass Air
Water Mass Flow Rate	kg/s	3.149E-02	3.149E-02	3.149E-02
Air Mass Flow Rate	kg/s	1.732E-03	3.465E-03	6.929E-03
Average Inlet Velocity (from CFD)	m/s	14.9	29.6	58.8
Inlet Pressure (from CFD)	bar <sub>g</sub>	0.289	0.603	1.32
Water Volume of Fluid Fraction	-	2.182E-02	1.103E-02	5.546E-03

Table 2. Parameter inputs and resulting inlet data from CFD simulations.



**Figure 6.** Sauter Mean Diameter (top) and velocity profiles (bottom) for all cases in x-axis.

Figures 6 and 7 show Sauter-Mean Diameter (SMD) and droplet velocity distributions along center x and y axes. From Figure 2 it can be noticed that as the AWMR is increased, the spray plume skews to the side. The resulting plume skewness is manifested in the in data presented in Figures 6-9 by both the PDI and LSI results.

It appears, in addition, that primary droplet breakup takes place prior the nozzle orifice. In PDI results, the detectable zones show that air caused the plume shift in x-axis especially in 20% Mass Air case, where detected region for drop size was only on the positive sides for both x and y axes. The drop size distribution was investigated in more detailed manner by plotting out the cumulative volume distributions along both x and y axes as shown in Figure 8. While overall drop size was based on volume flux weighting [3, 4], the data from Figure 8 was generated from PDI point measurements. These plots indicated that lower drop size range regions (generally middle of the covered spatial range) correlated with relatively higher droplet velocities (Figures 6 and 7), and with higher intensity shown by LSI measurements (Figure 9).

From figure 9, eccentricity of the spray plume in x direction was assessed visually. Based on this visual assessment Hydraulic case seems to be aligned closely with a nozzle. On the other hand, 20% Mass Air case seems to shift almost the whole spray plume across the x axis.

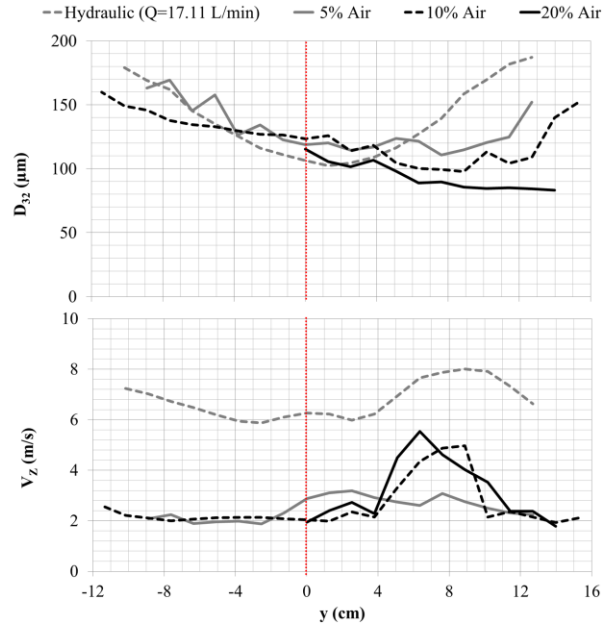


**Figure 7.** Sauter Mean Diameter (top) and velocity profiles (bottom) for all cases in y-axis

The shift of the spray plume is believed to be caused by the air-water mixture that forces itself to escape as fast as possible through the upper region of the nozzle helix following the path of least resistance. This creates an uneven distribution of flow is along the spiral. The higher the AWMR, the smaller the drops produced but this results in significant plume eccentricity.

## CFD Results

CFD was performed to investigate the velocity and water volume of fluid at the orifice (Figure 10). Also the iso-surfaces were created based on the half of the water VOF fraction value at the inlet (shown in table 2).

The exit velocities at the orifices were on the order of 50, 100 and 200 m/s for 5%, 10% and 20% AWMR, respectively. Since compressibility was not included in this set of simulations, the exit velocity values were proportional to mass flow rate of air.

Although the velocities and water VOF fractions were different at the orifice, the iso-surface shapes were quite similar (Figure 10). A change in shape is anticipated when the compressibility of air is included in future simulations.

Additionally, there are other things that should be considered in future simulations. One of them is surface tension with higher fidelity schemes. This kind of transient simulation (would probably require a demanding turbulence model) could help to determine the multi-phase nature of flow prior the injection, intermediate breakup at the orifice, assuming primary does occur prior injection, and finally secondary breakup.

## Conclusions

Spiral type nozzles are generally a deflecting type of nozzles designed to spray hydraulically. However, adding gaseous phase flow changes the nozzles' intended performance. This study has shown that drop size was reduced when air was added. However, the fast moving air-water mixture caused spray plume eccentricity. CFD gave an inside look at the scales of the velocities of air-water mixtures at the nozzle's orifice.

## References

1. Bachalo, W.D. and Houser, M.J., "Phase Doppler Spray Analyzer for Simultaneous Measurements of Drop Size and Velocity Distributions," *Optical Engineering*, Volume 23, Number 5, September-October, 1984.
2. Bachalo, W.D. and Houser, M.J., "Spray Drop Size and Velocity Measurements Using the Phase/Doppler Particle Analyzer", *Proceedings of the ICLASS (3rd Intl.)*, July 1985.
3. Bade, K. M., Schick, R. J., "Phase Doppler Interferometry Volume Flux Sensitivity to Parametric Settings and Droplet Trajectory", *Atomization and Sprays*, vol. 21, issue 7, p. 537-551, 2011.
4. Bade, K. M., Schick, R. J., "Post-Processing of Phase Doppler Interferometry Data for Planar Spray Characteristics", *ILASS-Americas conference*, Pittsburgh, PA, May 2013.
5. ANSYS FLUENT 14.5 - Theory Guide, ANSYS, Inc., Canonsburg, PA, 2012.

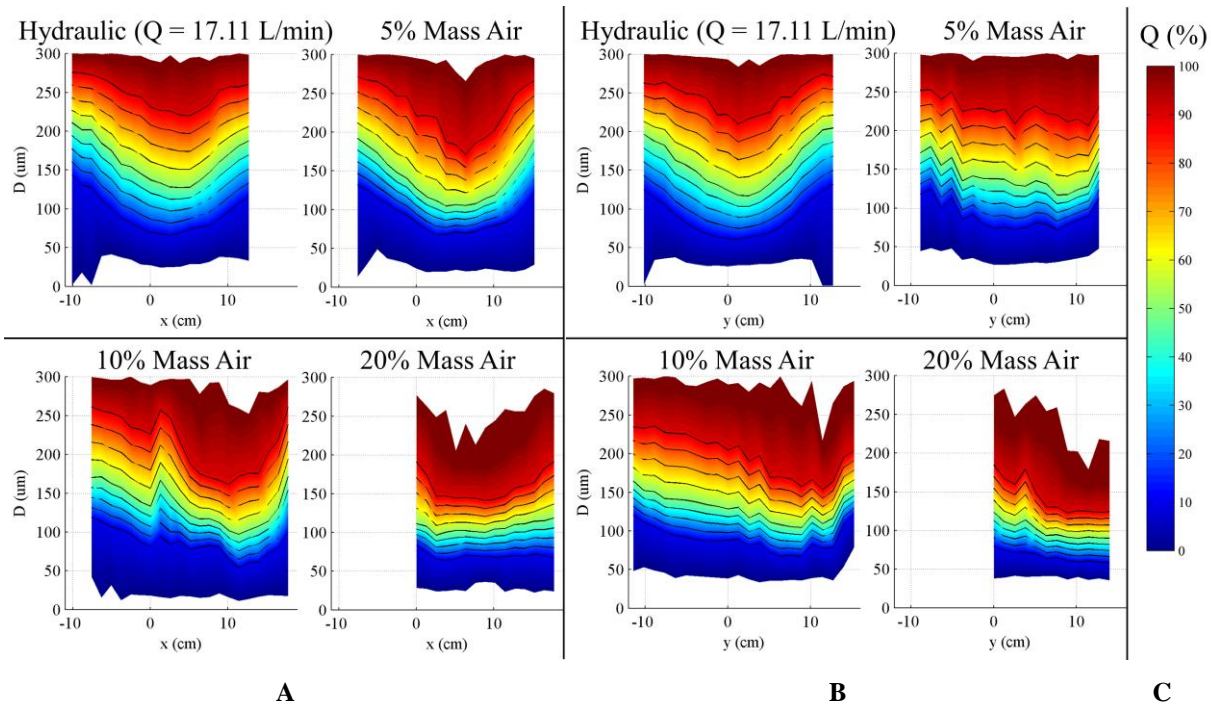


**Figure 8.** Drop size distribution along x-axis (A) and along y-axis (B) for all cases. Percentage of cumulative volume distribution was applied (C).

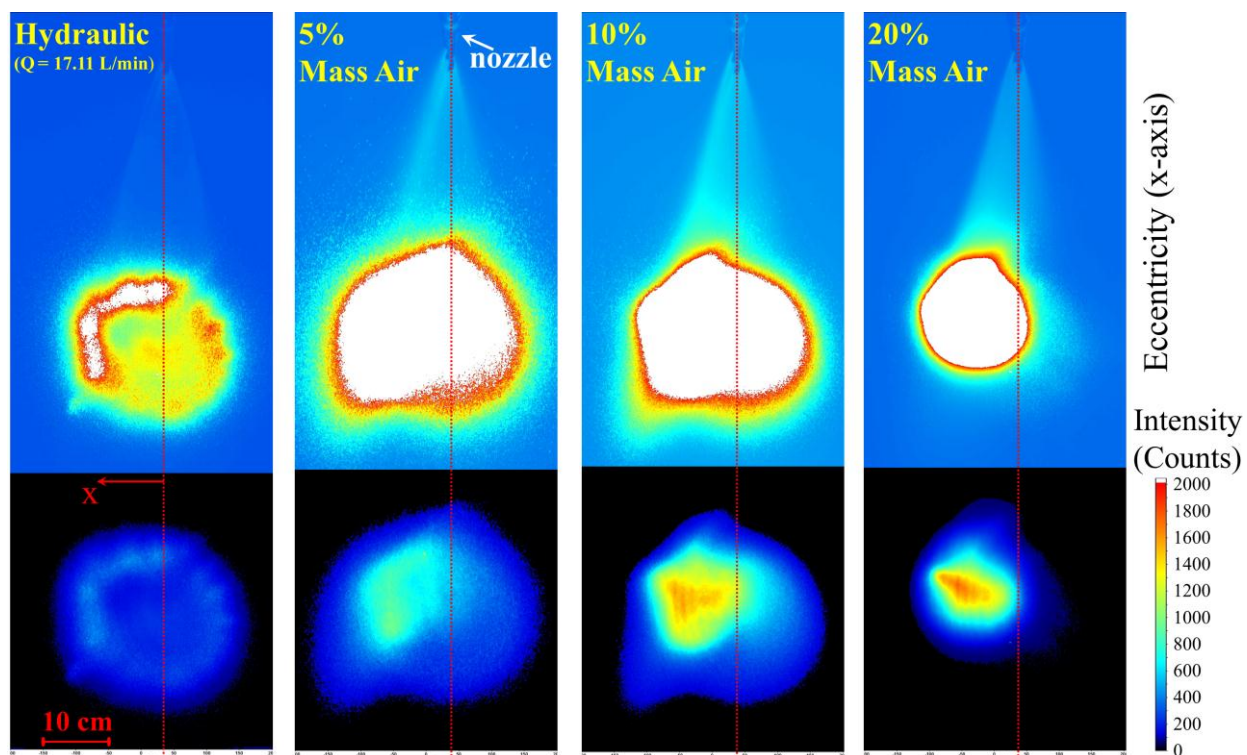


**Figure 9.** LSI results showing relative density distribution for all cases. Eccentricity in x-axis (top) and spray distribution at same intensity scale (bottom)

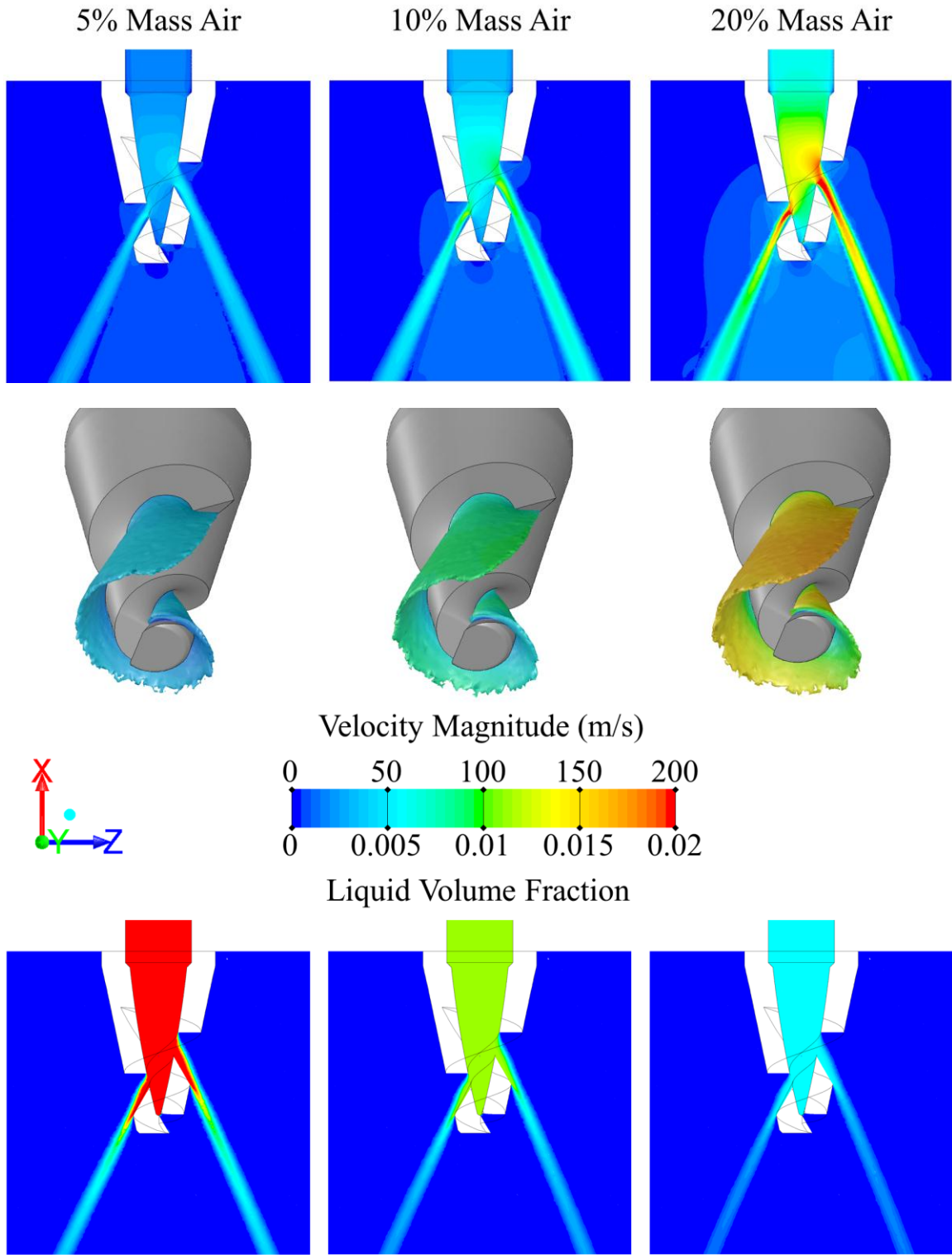


**Figure 10.** CFD results for 3 cases with different air/water mass flow ratios. Velocity contours (top), iso-surfaces of volume of fluid (middle), and volume of fluid contours (bottom),